Characteristics of Visible Fluorescence from Ionic Liquids

Seoncheol Cha,[†,‡] Taekyu Shim,[†] Yukio Ouchi,[§] and Doseok Kim*[,†,‡]

[†]Department of Physics and [‡]Research Institute for Basic Science, Sogang University, Seoul 121-742, Republic of Korea
[§]Department of Chemistry, Graduate School of Science, Nagoya University, Nagoya 464-8602, Japan

ABSTRACT: The observation of fluorescence in the visible spectral range in imidazolium-based ionic liquids, in which the peak of the fluorescence spectrum shifts with the change in the excitation wavelength by over 200 nm, was reported by Samanta and co-workers (Paul et al. *J. Phys. Chem. B* **2005**, *109*, 9148; *Chem. Phys. Lett.* **2005**, *402*, 375), and the aggregate structure in the bulk ionic liquid was suggested to explain this unique phenomenon. In this work, by employing 2D-scan fluorescence spectroscopy, we identified the long- and short-wavelength fluorescence components of the fluorescence spectrum of 1-butyl-3-methylimidazolium tetrafluoroborate ($[C_4MIM][BF_4]$), of which only the long-wavelength fluorescence component was found to be responsible for the reported fluorescence properties. The fluorescence intensity of the long-wavelength component decreased much faster upon dilution in aqueous mixtures than the short-wavelength component, supporting the conclusion that the long-wavelength fluorescence is from molecular aggregates in the bulk ionic liquid. Fluorescence correlation spectroscopy (FCS), which was used to accurately account for the number density of the long-wavelength fluorescent species in aqueous solutions of the ionic liquid, also suggested that the fluorescence came from aggregate structures of molecules in ionic liquids.
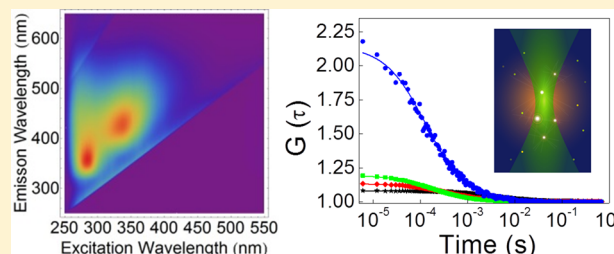
INTRODUCTION

Unusual absorption and fluorescence behavior in ionic liquids in the visible range has been reported.[1−6] The imidazolium-based ionic liquids for which this visible fluorescence was observed are expected to be transparent in the visible range because the electronic transition of the single 1-alkyl-3-methylimidazolium $[C_nMIM]$ core of the cation falls in the UV range (<300 nm).[7] Thus, the color often exhibited by some imidazolium-based ionic liquids was deemed to be from impurities, although definite chemical species were not identified.[8] Samanta and co-workers reported unusual long-tail absorption extending into the visible wavelength range of $[C_nMIM]$-cation ionic liquids, from which they also observed fluorescence in the visible range.[1−6] Unlike the fluorescence spectra of most organic molecules, which do not change with excitation wavelength (as is known by Kasha's rule),[9,10] the fluorescence from these ionic liquids has been shown to redshift continuously following the increase in the wavelength of the excitation beam. There have been suggestions that this novel fluorescence property of ionic liquids be applied in Förster resonance energy transfer experiments.[5,6]

To account for this visible absorption and emission from ionic liquids, some types of choromophoric impurities made during the synthesis process through alkylation by halides or introduced after synthesis have been proposed.[8,11] A substantial reduction in fluorescence intensity from pyrrolidinium ionic liquids was reported upon systematic purification of the precursor salts during synthesis.[12] Heating of imidazolium- and pyrrolidinium-based ionic liquids above 150 °C has been shown to increase the absorption and fluorescence in the visible range.[13] However, careful sample preparation and purification

have not usually improved the absorption in the visible tail part of the spectra, let alone allowed the identification of the responsible chemical species.[1,2] The heterogeneity in the bulk intermolecular structure was suggested to explain the novel fluorescent properties of ionic liquids.[1] Based on a study of $[C_4MIM][PF_6]$/acetonitrile mixtures at different concentrations, Samanta and co-workers suggested that the fluorescence originates from species in the ionic liquid having different electronic structures induced by the inherent heterogeneity of bulk ionic liquids.[1] Singh and Kumar measured the fluorescence, nuclear magnetic resonance (NMR), and Fourier transform infrared (FTIR) spectra of $[C_8mim][BF_4]$/ethylene glycol mixtures and suggested that molecular aggregates in ionic liquids are responsible for the fluorescence.[4]

An experiment needs to be designed to test the proposed mechanisms for this unique fluorescence behavior. Herein, we controlled the possible choromophoric impurities suspected for visible fluorescence on one hand and also investigated aqueous solutions of ionic liquids at different concentrations to see how the fluorescence changed upon dilution. Fluorescence correlation spectroscopy (FCS), which has been used to obtain the absolute concentrations and diffusion coefficients of fluorophores in solution by analyzing fluctuations in the fluorescence,[9,14,15] was employed in this study to suggest the origin of the visible fluorescence in pure ionic liquids. FCS on ionic liquid systems was first demonstrated by Baker and co-workers, who investigated the diffusion of dye molecules at

dilute concentrations with an ionic liquid as the solvent medium.[16] More recently, FCS was used to study the microscopic structural heterogeneity, such as self-aggregation or nonpolar domains, of ionic liquids by observing multiple diffusion coefficients of dyes dissolved in ionic liquids.[17−19] In a previous study, we found that FCS measurements of ionic liquids are possible without addition of any dye because of the fluorescence from the ionic liquid itself,[20] and the investigation was extended to aqueous solutions of ionic liquids to determine the origin of the fluorescence from the ionic liquids.

■ EXPERIMENTS

Ultrahigh-grade 1-butyl-*n*-methylimidazolium tetrafluoroborate ($[C_4MIM][BF_4]$) was purchased from C-TRI (Hwaseong City, Korea) and used without further purification. The chloride impurity in the purchased ionic liquid was less than 30 ppm, and the water impurity was less than 50 ppm. Ionic liquids having comparable grades from different manufacturers [FutureChem (Seoul, Korea) and Merck] showed the same fluorescence properties but differed slightly in terms of fluorescence intensities. The absorption spectra of our sample in Figure 1 show that the absorption of the sample used in this
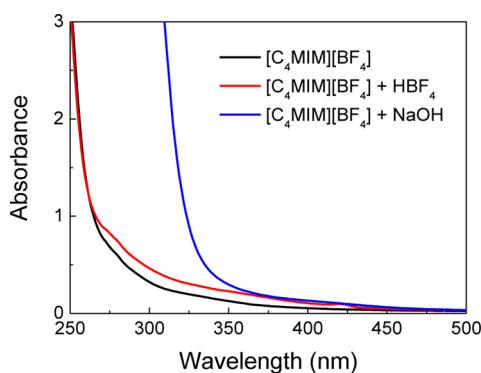

Figure 1. Absorption spectra of $[C_4MIM][BF_4]$ (black), $[C_4MIM]$-$[BF_4]$ + HBF_4 (red), and $[C_4MIM][BF_4]$ + NaOH (blue) (in 10-mm cuvettes).

study at the long-wavelength tail of the spectral band was comparable to or less than those from ionic liquids used in the previous studies.[1,2] Deionized water (18.2 MΩ·cm) was used to make ionic liquid/water mixtures. Ten microliters of 48 wt % HBF_4 (Aldrich) or 50% NaOH (Aldrich) solution was added to 4 mL of pure $[C_4MIM][BF_4]$ to change the proton concentration of the ionic liquid. Mixture solutions were made by stirring with magnetic stirrer for more than 12 h.

Quartz and synthetic quartz cuvettes (Hellma, 10 mm) were used to measure UV−visible absorption and fluorescence spectra. UV−visible absorption spectra were measured with HP 2942A and JASCO J-330 UV−visible absorption spectrometers. Fluorescence and 2D-scan fluorescence spectra were measured with a Hitachi F-1100 spectrofluorometer. The excitation and emission slit widths of the spectrofluorometer were either 2.5 or 10 nm, and the spectra were found to be similar between these two slit widths. All measurements were performed at room temperature (25 °C). The frequency-doubled beam of a Ti:sapphire laser output (800 nm, 100 fs pulse width, 82 MHz repetition rate) was used to excite $[C_4MIM][BF_4]$ for fluorescence decay time measurements. The collected fluorescence signal was filtered by a monochromator (MS3504i, SOLAR TII) and detected by a microchannel plate photo-

multiplier tube (R3809U-51, Hamamatsu). A time-correlated single-photon-counting (TCSPC) board (SPC-730, Becker & Hickl GmbH) was used to obtain the fluorescence decay time profile.

The FCS setup was based on a home-built confocal microscope.[21] The 532-nm laser beam used as the excitation source was focused with a water-immersion objective lens (NA = 1.2, Olympus) on the sample. Tetramethyl rhodamine (TMR) dye was used for calibration of the confocal detection volume. Fluorescence was collected with the same objective lens, separated from the excitation light by a dichroic mirror, and sent to a bandpass filter (585-40, Semrock, OD > 6.5 at 532 nm) to further block the scattered pump light from the solvent. The number of fluorescence counts measured was between 1000 and 50000 counts/s depending on the IL concentration. When water was put in the sample chamber to check for the amount of scattered light that might leak through the fluorescence filter, the photon count dropped to the dark count of the avalanche photodiode (APD) (∼400 counts/s) used in the setup. The fluorescence was then focused by lens to an optical fiber (62.5-μm in diameter) used as a confocal pinhole to eliminate the background from the out-of-focus region. The fluorescence photon counts were simultaneously recorded during the FCS measurements.

The confocal detection volume of ∼1 fL is small enough to have only a few molecules in it at a dye concentration of ∼1 nM. Brownian motion of these dye molecules into and out of the confocal detection volume in the sample causes fluctuations in the fluorescence intensity. The time correlation function of these intensity fluctuations is analyzed by the single-species free diffusion model as follows[9,14,15]

$$G(\tau) = \frac{\langle \delta F(t) \cdot \delta F(t+\tau) \rangle}{\langle F(t) \rangle^2}$$

$$= \frac{1}{\bar{N}}\left(1 + \frac{\tau}{\tau_d}\right)^{-1}\left[1 + \left(\frac{w_{xy}^2}{w_z^2}\right)^2 \frac{\tau}{\tau_d}\right]^{-1/2} \quad (1)$$

where $\delta F = F(t) - \langle F(t) \rangle$; $\langle F(t) \rangle$ is the time-average of the fluorescence intensity; $\tau_d = w_{xy}^2/4D$; and w_{xy} and w_z are the lateral and longitudinal distances (distance from the focal point at which the intensity drops to $1/e^2$ of its maximum value), respectively. N is the average number of dye molecules in the confocal volume, and D is the diffusion coefficient. The excitation power was kept below 200 μW to avoid optical saturation effects during FCS measurements.

■ RESULTS AND DISCUSSION

Ionic liquids having $[C_nMIM]$ cations are expected to be transparent in the visible range, as the electronic absorption of the single imidazolium core falls below the UV range (<300 nm).[7] The actual absorption spectra of ionic liquids having $[C_nMIM]$ cations, however, exhibit weak absorption extending into the visible range.[1−4] Figure 1 shows the absorption spectrum of $[C_4MIM][BF_4]$ as an example, showing the tail in the absorption band extending up to ∼500 nm. For the pure $[C_4MIM][BF_4]$ used in our study (black line in Figure 1), the absorption at the tail after the absorption edge is smaller than those from previous reports,[1,2] in which the sample was purified extensively postsynthesis. Thus, the relative purity of our ionic liquid can be assured. The absorption spectra of $[C_4MIM]$-
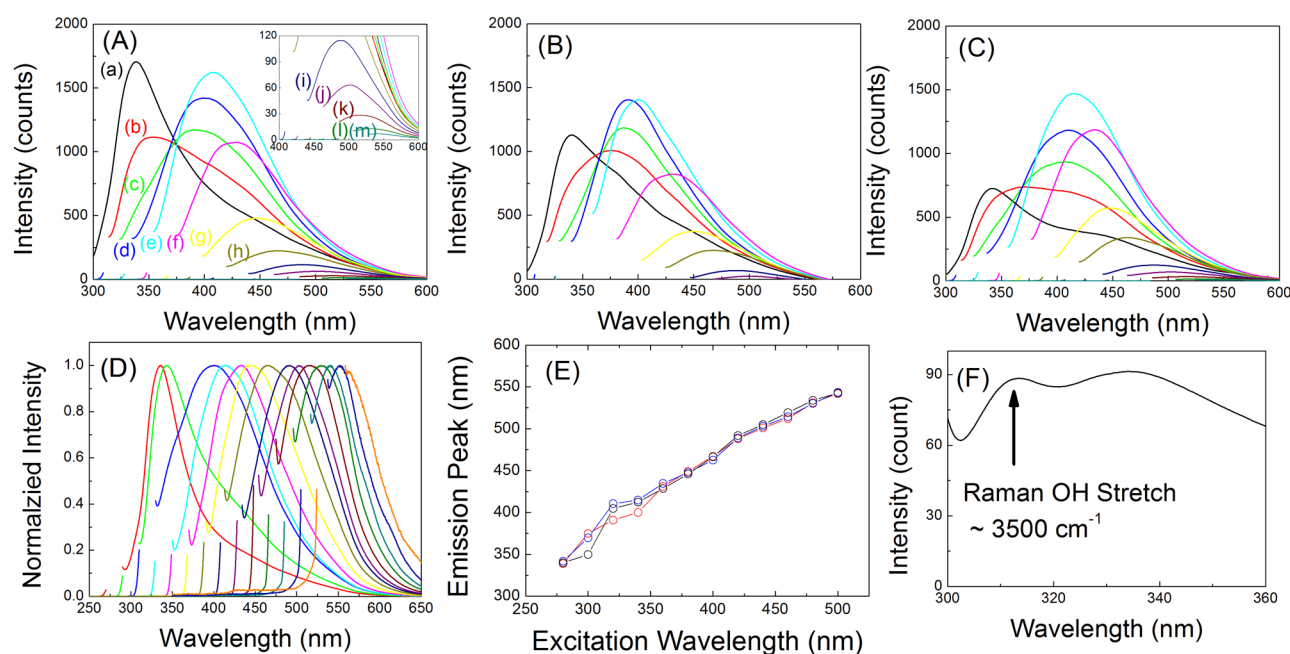
Figure 2. Fluorescence spectra of (A) pure $[C_4MIM][BF_4]$, (B) $[C_4MIM][BF_4]$ + HBF_4, (C) $[C_4MIM][BF_4]$ + NaOH, and (D) pure $[C_4MIM][BF_4]$ (normalized) excited by lights at different wavelengths: (a) 280, (b) 300, (c) 320, (d) 340, (e) 360, (f) 380, (g) 400, (h) 420, (i) 440, (j) 460, (k) 480, (l) 500, and (m) 520 nm. (E) Peak shift versus excitation wavelength from pure $[C_4MIM][BF_4]$ (black), $[C_4MIM][BF_4]$ + HBF_4 (red), and $[C_4MIM][BF_4]$ + NaOH (blue). (F) Fluorescence spectrum of an aqueous solution of $[C_4MIM][BF_4]$ at 0.05 M concentration, excited at 280 nm.

$[BF_4]$ + HBF_4 and $[C_4MIM][BF_4]$ + NaOH will be discussed later, together with their fluorescence properties.

Panels A and D of Figure 2 show fluorescence spectra of $[C_4MIM][BF_4]$ obtained at different excitation wavelengths from 280 to 500 nm. Hereafter, we investigated only $[C_4MIM][BF_4]$ because imidazolium-based ionic liquids having different cations and anions showed very similar fluorescence behaviors.[1,2,4] The fluorescence spectra continuously change in shape and the overall intensity decreases with increasing excitation-beam wavelength.[1–6] The spectral band is not due to Raman-scattered light because the emission bandwidth of the spectrum is much wider than the spectrum expected from the Raman scattering, and the shift of the fluorescence peak position does not follow the change in excitation photon energy (Figure 2E), as reported previously.[1,2]

The fluorescence was not very strong but was easily detectable, especially when excited by a short wavelength. To give a quantitative idea of the fluorescence intensity, the fluorescence signal from a 0.05 M aqueous solution of $[C_4MIM][BF_4]$ was comparable to the Raman-scattering signal from the OH-stretching mode of water measured by filling the same cuvette with water, upon excitation at 280 nm and measured by the same spectrometer (Figure 2F). As another measure, the fluorescence intensity of pure $[C_4MIM][BF_4]$ was slightly (∼20%) brighter than the fluorescence from 1 nM TMR dye in our confocal microscope setup upon excitation at 532 nm.

As is evident from Figure 2D, the fluorescence spectrum of $[C_4MIM][BF_4]$ violates Kasha's rule, which states that the fluorescence spectra of organic molecules should not change with a change in the excitation wavelength. A peak shift of up to a few nanometers following a change in the excitation-beam wavelength, in violation of Kasha's rule, was observed from conventional chromophores because of the slow dynamics of

these viscous solvents and is termed the "red-edge effect".[9,22,23] Recently, the red-edge effect was also observed in ionic liquids, in which fluorescence spectra from organic dye molecules dissolved in ionic liquids shifted a bit more than in the previous reports on viscous organic solvents.[3,22,24–28] By contrast, the fluorescence peak shifts observed in the pure ionic liquids are greater than 200 nm (Figure 2E), which suggests that the responsible mechanism is different from that occurring in previous cases.

As the imidazolium core of the $[C_nMIM]$ cation cannot support absorption and fluorescence emission at visible wavelengths, the possibility of impurities with energy levels in the visible range can be considered. Among the candidates for impurities, the deprotonated form of the imidazole cation in which the most acidic proton attached to the C(2) (carbon between the two nitrogens) is deprotonated to yield a neutral carbon atom with lone-pair electrons is known to be highly reactive in the formation of imidazole dimer.[29] This imidazole dimer has a longer electron conjugation length than the single imidazole core and can possibly account for the long-wavelength absorption and emission observed.

To check for the possibility of imidazole dimers as fluorescent species, the acidity (or proton concentration) of the bulk $[C_4MIM][BF_4]$ was changed intentionally by adding HBF_4 or NaOH. Upon the addition of 10 μL of HBF_4 or NaOH to 4 mL of pure $[C_4MIM][BF_4]$, the infrared absorption spectra did not change much, as, presumably, the amounts of NaOH or HBF_4 added were not enough to show appreciable changes in the infrared spectra in the 1000–4000 cm^{-1} range. By contrast, the change in the UV–visible absorption was easily detectable. Figure 1 shows the UV–visible absorption spectrum of pure $[C_4MIM][BF_4]$ together with those of $[C_4MIM][BF_4]$ + HBF_4 and $[C_4MIM][BF_4]$ + NaOH. When NaOH was added to promote the formation of carbene (and the imidazole

dimer), the adsorption edge moved ~50 nm to the red. The difference in the absorption can be attributed to the electronic absorption from the imidazole dimer. We expected the absorption at the tail to decrease when HBF_4 was added, as HBF_4 would work to decrease the imidazole dimers in $[C_4MIM][BF_4]$, but the absorption at the tail increased, albeit very slightly. The species responsible for this small changes are unknown, but such small changes despite the increase of the proton concentration should indicate that the initial $[C_4MIM]$-$[BF_4]$ used in this study was very pure, free from imidazole dimers.

Afterward, the fluorescence characteristics of the same samples were investigated. Panels B and C of Figure 2 are the excitation-wavelength-dependent emission spectra from $[C_4MIM][BF_4]$ with addition of HBF_4 and NaOH, respectively. Figure 2E shows the excitation wavelengths versus the emission peak positions. The emission peak positions are almost similar for the three samples, showing that the excitation wavelength dependence of the fluorescence does not change much under acidic or basic environments. As the fluorescence properties including overall fluorescence intensity, peak shift, and spectral shape did not change much upon addition of HBF_4 and NaOH to change carbene dimer impurities, it was concluded that the imidazole dimer is not responsible for the fluorescence from pure ionic liquids.

To study the fluorescence characteristics of $[C_4MIM][BF_4]$ in more detail, 2D-scan fluorescence spectroscopy was employed. The usual florescence spectrum is measured at a fixed excitation wavelength, whereas the photoluminescence excitation (PLE) spectrum is obtained by scanning the excitation wavelength while measuring the fluorescence intensity at a fixed emission wavelength. For 2D-scan fluorescence measurements, fluorescence spectra are measured as the excitation wavelength is scanned to monitor the fluorescence behavior more clearly.

The 2D-scan fluorescence spectrum from pure $[C_4MIM]$-$[BF_4]$ in Figure 3 showed two distinct peaks. The first peak in

Figure 4. (A) Fluorescence and (B) normalized fluorescence spectra of aqueous solutions of $[C_4MIM][BF_4]$ at different concentrations: (from top to bottom) pure $[C_4MIM][BF_4]$ (5.27 M) and 1.07, 0.51, 0.30, 0.15, and 0.05 M. The excitation wavelength was 280 nm.

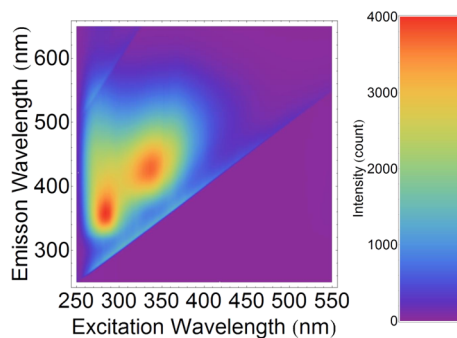**Figure 3.** Contour map of 2D-scan fluorescence spectra of $[C_4MIM][BF_4]$. The bright lines, namely, the one across the center of the figure (with slope 1) and the one at the upper left corner (with slope 2), are due to elastically scattered pump lights from the grating (first- and second-order).

the short-wavelength range (in the lower left corner) centered around 350 nm disappears for pump wavelengths longer than 300 nm. This peak is elongated along the vertical direction, indicating that the spectral shape and peak position do not change with the excitation wavelength. The other peak at longer wavelength is clearly separated from the short-wavelength peak. As this peak is elongated along the diagonal

direction, the corresponding fluorescence band would redshift with a change in the excitation-beam wavelength. The distinct shapes described above and the clear spectral separation of these two peaks suggest that the origins of fluorescence from these bands are different.

Fluorescence spectra were then measured for water/$[C_4MIM][BF_4]$ mixtures at different concentrations to see how the two peaks in the 2D-scan fluorescence spectra change with conce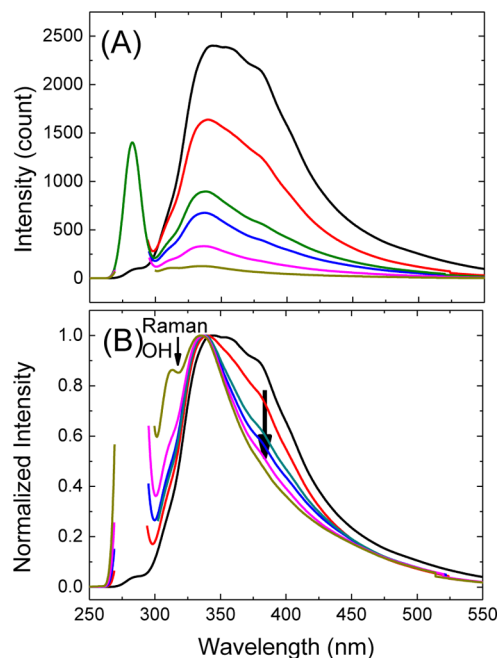ntration. In Figure 4, the peak at 280 nm is elastically scattered pump light, whereas the second shorter-wavelength peak (~310 nm), shown only in much-diluted concentrations of $[C_4MIM][BF_4]$, is Raman-scattered light from the OH-stretching modes of water. The strongest peak around 350 nm corresponds to the short-wavelength peak of $[C_4MIM][BF_4]$ found from the 2D spectra in Figure 3. This short-wavelength peak from the water/$[C_4MIM][BF_4]$ mixture system decreases in intensity upon dilution of $[C_4MIM][BF_4]$, whereas the long-wavelength shoulder of the peak decreases much faster upon dilution, as evidenced in Figure 4B. This result is consistent with the result of Samanta and co-workers, in which they measured the fluorescence spectra for $[C_4MIM][PF_6]$/acetonitrile mixtures at different concentrations.[1] A faster decrease of the long-wavelength peak or shoulder upon dilution as compared to the short-wavelength peak was seen, from which they inferred that the fluorescence at the long-wavelength peak cannot be from a single $[C_4MIM]$ cation, but could possibly be due to higher structures such as molecular aggregates.

Plotted in Figure 5 are the peak intensity changes with concentration from the fluorescence spectra of water/$[C_4MIM][BF_4]$ mixtures at different excitation wavelengths. The 2D-scan fluorescence result in Figure 3 shows that the first peak changes to the second peak without much coexistence of the two peaks under one fluorescence spectrum; thus, we
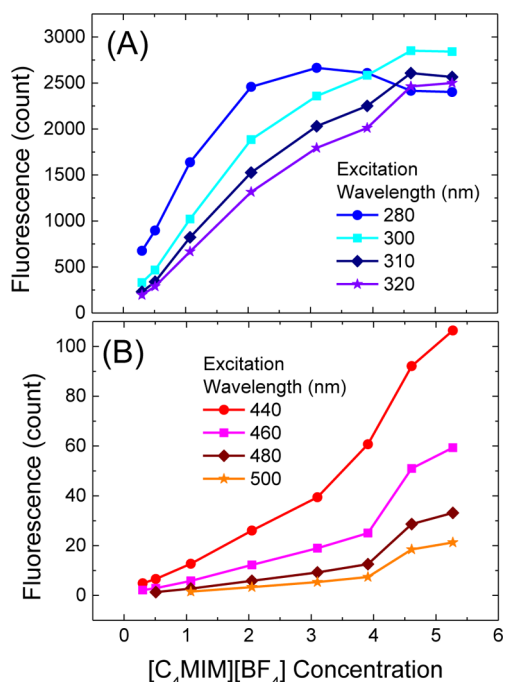
Figure 5. Fluorescence intensity vs concentration for water/[C$_4$MIM][BF$_4$] mixtures upon (A) short- and (B) long-wavelength excitation.

divided our data into two groups to show short-wavelength excitations in Figure 5A and long-wavelength excitations in Figure 5B. The fluorescence spectra with excitation around 400 nm were not analyzed, as (1) the overlapping between Raman scattering from OH vibration mode and the fluorescence peak and (2) the appearance of both short- and long-wavelength bands complicated the analysis. The intensity change upon short-wavelength excitations (Figure 5A) shows a slow decrease with decreasing ionic liquid concentration. By contrast, the intensity decrease in Figure 5B is much faster than linear, with a significant drop at around 4 M, confirming the faster decay at the long-wavelength shoulder, as shown in Figure 4B. This behavior lends support for the proposition that the long-wavelength fluorescence is from molecular aggregates.

The fluorescence intensity cannot accurately account for the number of fluorophores in the mixture, because the extinction coefficient and quantum yield of the fluorophores can also change with the mixture concentration. To overcome this difficulty, FCS is an ideal technique for determining low levels

of fluorophore concentrations in solution. FCS employs the intensity correlation function to analyze temporal fluctuations of the fluorescent intensity arising from the diffusional motion of fluorophores into and out of a small volume of the confocal microscope to determine the concentration of the fluorophores. Particularly for the single-species free diffusion case, FCS is free from other effects such as the extinction coefficient, the quantum yield of the fluorophore, and the excitation power.

A 532-nm laser was used to excite only the long-wavelength fluorescence species in Figure 3. Figure 6A is a steady-state fluorescence spectrum excited at 532 nm to show the long-wavelength emission of the ionic liquid in this range obtained by the same spectrofluorometer as used in Figure 2A. In the actual FCS measurements, a bandpass filter (passing range of 565−605 nm) was used in the detection beam path to send only the fluorescence output to the APD for FCS measurements, while blocking the scattered pump light very effectively. Figure 6B shows the fluorescence decay profile from pure [C$_4$MIM][BF$_4$] measured by the TCSPC technique to ensure that the measured signal was not scattered pump light but, was from the electronic transition in the fluorophore. The decay profile could be fitted by two exponential functions having decay times of 400 ps and 3.5 ns, in good agreement with the previous reports,[1] whereas the long-lifetime (∼10 ns) component could not be measured because of the high repetition rate (82 MHz) of the laser.

As already shown in our previous reports,[20] the correlation functions obtained by FCS measurements on pure ionic liquids ([C$_4$MIM][BF$_4$], [C$_4$MIM][PF$_6$], and [C$_8$MIM][BF$_4$]) were fitted reasonably well with the single-species free diffusion model. The concentration of the fluorescent species in the ionic liquid deduced from the amplitude of the measured fluorescence correlation function fell in the range of 10−30 nM,[20] making it possible to apply this technique to determine the concentration of fluorophores for dilute mixtures. This low concentration indicates that the origin of the long-wavelength fluorescence is not the single cation or single ion pair, which are much more abundant inside the focal volume, but either a trace amount of the impurities or a particular structure of molecular aggregates that can fluoresce in the visible range. Concentration dependence measurements were performed to identify one of the two possibilities.

Figure 7 shows the correlation functions obtained from aqueous solutions of [C$_4$MIM][BF$_4$]. The correlations functions were well fitted by the single-species free diffusion model in eq 1. $G(0)$ (the height of the correlation function at τ
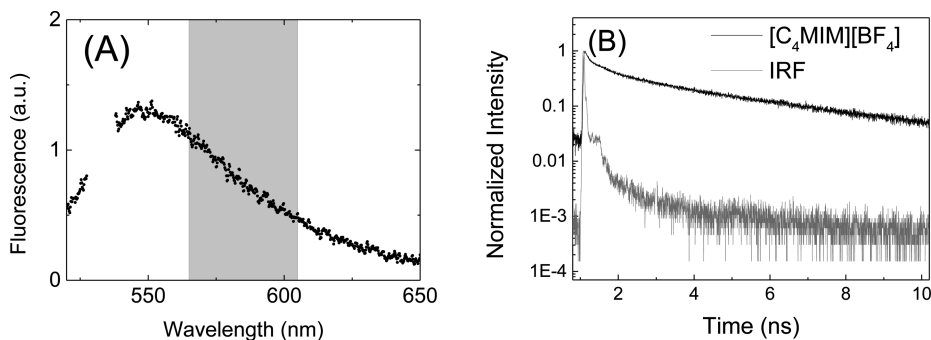

Figure 6. (A) Steady-state fluorescence spectrum of [C$_4$MIM][BF$_4$] excited at 532 nm and measured by spectrofluorometer. The gray box indicates the transmission range of the bandpass filter used in the FCS setup. (B) (black) Fluorescence decay profile of [C$_4$MIM][BF$_4$] and (gray) instrumental response function (IRF) of the microchannel plate photomultiplier tube. The sample was excited at 400 nm and measured at 580 nm.
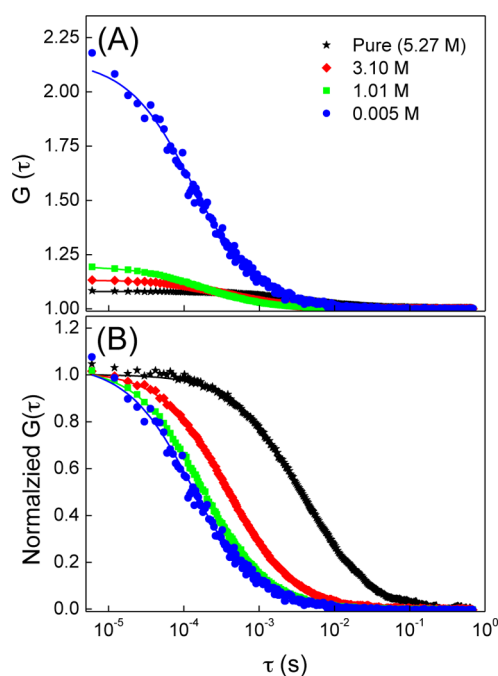
Figure 7. (A) Fluorescence correlation functions and (B) normalized correlation functions of aqueous solutions of $[C_4MIM][BF_4]$ at different concentrations as determined by FCS:(from bottom to top for panel A and from right to left for panel B) pure $[C_4MIM][BF_4]$ (5.27 M) and 3.10, 1.01, and 0.005 M. Solid lines are fits with the single-species model.

= 0) is inversely proportional to the number of fluorophore in the sample, and $G(0)$ in Figure 7A increases upon dilution of the ionic liquid sample, indicating that the number of fluorophores decreased as the water content increased. The diffusion time τ_d for which $G(\tau_d) \approx {}^1/_2 G(0)$ is the average residence time of the fluorophore in the focal volume and is inversely proportional to the diffusion coefficient of the sample. The normalized correlation traces in Figure 7B show that the diffusion time τ_d decreased with increasing water content in the sample.

The concentrations of the fluorophores deduced from the amplitudes of the fitted correlation function $G(0)$ of the mixtures at different concentrations are shown in Figure 8. If the fluorescence is from impurities in the ionic liquid (introduced during the synthesis procedure or by contami-
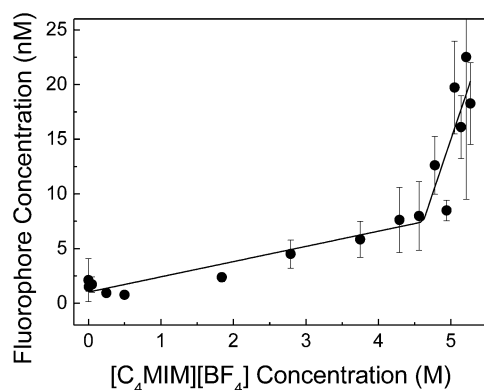

Figure 8. Fluorophore concentration vs $[C_4MIM][BF4]$ concentration in solution. The lines are linear fits to the data.

nation), the fluorescence intensity would have a linear dependence with the change in the concentration of ionic liquid in the mixture. On the contrary, the concentration of the fluorophore determined from FCS showed an abrupt change in slope at around 4.5 M. This concentration dependence indicates that the fluorescent species in $[C_4MIM][BF_4]$ is somehow broken by the introduction of water and strongly suggests that molecular aggregates of the ionic liquids are the fluorescent species.

The hydrodynamic radius of the fluorescent species could also be estimated from the FCS results by using eq 1. The diffusion coefficients of the fluorescence species in the mixture (D_F) is shown to decrease in Figure 9 with increasing ionic
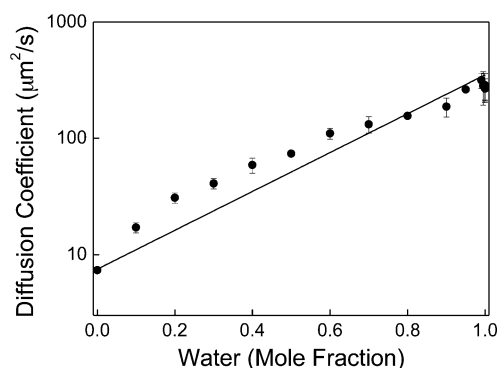

Figure 9. Diffusion coefficients of the fluorophores in aqueous solutions (D_F) of $[C_4MIM][BF_4]$ deduced by fitting the fluorescence correlation functions. The solid line is an exponential fit with exponent $a = 0.26$ in eq 3.

liquid concentration. Now, D_F can be expressed in terms of the viscosity of the ionic liquid/water mixture using the Stokes−Einstein relation. The viscosity of the aqueous solution of $[C_4MIM][BF_4]$ is known to decrease exponentially upon addition of water as follows[30]

$$\eta = \eta_0 \exp(-x_{cs}/a) \qquad (2)$$

where η is the viscosity of the aqueous solution of ionic liquid, η_0 is the viscosity of pure ionic liquid, x_{cs} is mole fraction of water, and a is a phenomenological constant (0.23 for $[C_4MIM][BF_4]$).[30] Thus, using the simplifying assumption that the hydrodynamic radius of the fluorophore does not change with concentration, the diffusion coefficient of the fluorophore in the solution should be inversely proportional to the viscosity of the water/ionic liquid mixture as follows

$$D_F = D_0 \exp(x_{cs}/a) \qquad (3)$$

where $D_0 = 7.5$ $\mu m^2/s$ is the diffusion coefficient of the fluorophore in pure $[C_4MIM][BF_4]$ and $a = 0.26$ to best fit our data. Using the Stokes−Einstein relation, the hydrodynamic radius of the fluorophore ranges from 1.3 to 2.6 Å depending on the reported viscosity values of pure $[C_4MIM][BF_4]$ (110−219 cP).[30−34] The values obtained by FCS were much smaller than the size of aggregates suggested by molecular dynamic simulations for $[C_nMIM][PF_6]$ (11−20 Å), by an X-ray scattering study of $[C_nMIM][Cl]$ (13−27 Å), or by small-angle neutron scattering of aqueous solutions of $[C_4MIM]$-$[BF_4]$ (8.5−13.5 Å),[35−37] let alone the size of a single $[C_4MIM]$ cation (∼5 Å).

Difficulties in determining the size of the diffusing species in an ionic liquid by using Stokes−Einstein relation have been

reported previously.[38−43] Umecky et al. measured the self-diffusion coefficient of $[C_4MIM][PF_6]$ by using the spin−echo NMR technique to deduce the hydrodynamic radius of the cation and anion.[41] The hydrodynamic radius from their study was also ∼3 times smaller than the radius suggested from the van der Waals volume of $[C_4MIM][PF_6]$. As related findings, molecular dynamics simulations and spin−echo NMR experiments suggested that the cations have much faster diffusional motion than the anions even though their van der Waals volumes are appreciably larger than those of the anions.[39,40,42,43] For example, the radius of the $[C_4MIM][BF_4]$ cation (∼3.3 Å) is larger than that of the anion (∼2.2 Å), but the cations were found to diffuse ∼50% faster than the anions.[39] For imidazolium ionic liquids having the same cation and different anions, the anion size did not show a clear correlation with the hydrodynamic radius by the Stokes−Einstein relation and spin−echo measurements.[38] From electrochemical measurements of haloaluminate ionic liquids, the diffusion coefficients of different ions having the same charge were found to be very similar despite their different ionic sizes (e.g., $[Re_2Cl_8]^{3-}$ and $[Re_3Cl_{12}]^{3-}$).[44] These studies that reported the size anomaly in the ionic liquids could be related to the unexpected small hydrodynamic radius found in our FCS measurements.

These studies that witnessed the failure of Stokes−Einstein relation in ionic liquids suggest that the Coulomb interaction between the ions, not just the size, is important in the diffusional motion in ionic liquids. It can also be imagined that the viscosity measured by FCS and the spin−echo NMR technique could be different from the macroscopic viscosity measured by typical viscometers. Indeed, differences in the diffusion phenomena at the microscopic and macroscopic scales are known.[45] The microscopic structural heterogeneity of ionic liquids might account for the differences between microscopic and macroscopic diffusion,[17,24,25,36,46] which can be investigated further using different methods in the future.

CONCLUSIONS

The unusual fluorescence from $[C_4MIM][BF_4]$ was investigated by steady-state fluorescence and FCS to find out the origin of fluorescence from pure ionic liquid. The fluorescence peak shift of over ∼200 nm following a change in the excitation wavelength confirmed the previous findings.[1,2] Addition of acid or base to pure $[C_4MIM][BF_4]$ did not change the fluorescence characteristics appreciably from those of pure $[C_4MIM][BF_4]$, demonstrating that the fluorescence is not from imidazole dimers. The short-wavelength fluorescence (at ∼360 nm) is considered to come from single molecules, whereas the long-wavelength fluorescence component was clearly distinguished by its separate peak position in the 2D-scan fluorescence spectrum, as well as its faster decrease in fluorescence intensity under dilution in aqueous mixtures. FCS was used to identify the long-wavelength species by measuring the concentration dependence of the fluorescence intensity. Fluorophore concentration determined by FCS decreases faster than dilution, indicating that the long-wavelength fluorescent species are broken by water, which gave strong experimental support for molecular aggregates as the source of the unique fluorescence properties of ionic liquids.[1,4]

AUTHOR INFORMATION

Corresponding Author
*E-mail: doseok@sogang.ac.kr; Fax: +82-2-7114518; Phone: +82-2-7058878.

Notes
The authors declare no competing financial interest.

REFERENCES

(1) Paul, A.; Mandal, P. K.; Samanta, A. On the Optical Properties of the Imidazolium Ionic Liquids. *J. Phys. Chem. B* **2005**, *109*, 9148−9153.

(2) Paul, A.; Mandal, P. K.; Samanta, A. How Transparent are The Imidazolium Ionic Liquids? A Case Study with 1-Methyl-3-butylimidazolium Hexafluorophosphate, [bmim][PF₆]. *Chem. Phys. Lett.* **2005**, *402*, 375−379.

(3) Mandal, P. K.; Paul, A.; Samanta, A. Excitation Wavelength Dependent Fluorescence Behavior of the Room Temperature Ionic Liquids and Dissolved Dipolar Solutes. *J. Photochem. Photobiol. A* **2006**, *182*, 113−120.

(4) Singh, T.; Kumar, A. Fluorescence Behavior and Specific Interactions of an Ionic Liquid in Ethylene Glycol Derivatives. *J. Phys. Chem. B* **2008**, *112*, 4079−4086.

(5) Izawa, H.; Wakizono, S.; Kadokawa, J. Fluorescence Resonance-Energy-Transfer in Systems of Rhodamine 6G with Ionic Liquid Showing Emissions by Excitation at Wide Wavelength Areas. *Chem. Commun.* **2010**, *46*, 6359−6361.

(6) Chen, X. W.; Liu, J. W.; Wang, J. H. A Highly Fluorescent Hydrophilic Ionic Liquid as a Potential Probe for the Sensing of Biomacromolecules. *J. Phys. Chem. B* **2011**, *115*, 1524−1530.

(7) Katoh, R. Absorption Spectra of Imidazolium Ionic Liquids. *Chem. Lett.* **2007**, *36*, 1256−1257.

(8) Earle, M. J.; Gordon, C. M.; Plechkova, N. V.; Seddon, K. R.; Welton, T. Decolorization of Ionic Liquids for Spectroscopy. *Anal. Chem.* **2007**, *79*, 758−764.

(9) Lakowicz, J. R. *Principles of Fluorescence Spectroscopy*, 3rd ed.; Springer: New York, 2006.

(10) Valeur, B. *Molecular Fluorescence: Principles and Applications*; Wiley-VCH: Weinheim, Germany, 2002.

(11) Anderson, J. L.; Ding, J.; Welton, T.; Armstrong, D. W. Characterizing Ionic Liquids on the Basis of Multiple Solvation Interactions. *J. Am. Chem. Soc.* **2002**, *124*, 14247−14254.

(12) Burrell, A. K.; Del Sesto, R. E.; Baker, S. N.; McCleskey, T. M.; Baker, G. A. The Large Scale Synthesis of Pure Imidazolium and Pyrrolidinium Ionic Liquids. *Green Chem.* **2007**, *9*, 449−454.

(13) Del Sesto, R. E.; McCleskey, T. M.; Macomber, C.; Ott, K. C.; Koppisch, A. T.; Baker, G. A.; Burrell, A. K. Limited Thermal Stability of Imidazolium and Pyrrolidinium Ionic Liquids. *Thermochim. Acta* **2009**, *491*, 118−120.

(14) Magde, D.; Elson, E.; Webb, W. W. Thermodynamic Fluctuations in a Reacting System—Measurement by Fluorescence Correlation Spectroscopy. *Phys. Rev. Lett.* **1972**, *29*, 705−708.

(15) Krichevsky, O.; Bonnet, G. Fluorescence Correlation Spectroscopy: The Technique and Its Applications. *Rep. Prog. Phys.* **2002**, *65*, 251−297.

(16) Werner, J. H.; Baker, S. N.; Baker, G. A. Fluorescence Correlation Spectroscopic Studies of Diffusion within the Ionic Liquid 1-Butyl-3-methylimidazolium Hexafluorophosphate. *Analyst* **2003**, *128*, 786−789.

(17) Guo, J. C.; Baker, G. A.; Hillesheim, P. C.; Dai, S.; Shaw, R. W.; Mahurin, S. M. Fluorescence Correlation Spectroscopy Evidence for Structural Heterogeneity in Ionic Liquids. *Phys. Chem. Chem. Phys.* **2011**, *13*, 12395−12398.

(18) Patra, S.; Samanta, A. Microheterogeneity of Some Imidazolium Ionic Liquids As Revealed by Fluorescence Correlation Spectroscopy and Lifetime Studies. *J. Phys. Chem. B* **2012**, *116*, 12275−12283.

(19) Sasmal, D. K.; Mandal, A. K.; Mondal, T.; Bhattacharyya, K. Diffusion of Organic Dyes in Ionic Liquid and Giant Micron Sized Ionic Liquid Mixed Micelle: Fluorescence Correlation Spectroscopy. *J. Phys. Chem. B* **2011**, *115*, 7781−7787.

(20) Cha, S.; Kim, D. Fluorescence Correlation Spectroscopy Study on Room-Temperature Ionic Liquids. *J. Korean Phys. Soc.* **2012**, *61*, 1555−1559.

(21) Cha, S.; Kim, S. H.; Kim, D. Viscosity of Sucrose Aqueous Solutions Measured by Using Fluorescence Correlation Spectroscopy. *J. Korean Phys. Soc.* **2010**, *56*, 1315−1318.

(22) Shim, T.; Lee, M. H.; Kim, D.; Ouchi, Y. Comparison of Photophysical Properties of the Hemicyanine Dyes in Ionic and Nonionic Solvents. *J. Phys. Chem. B* **2008**, *112*, 1906−1912.

(23) Demchenko, A. P. The Red-Edge Effects: 30 Years of Exploration. *Luminescence* **2002**, *17*, 19−42.

(24) Hu, Z. H.; Margulis, C. J. Heterogeneity in a Room-Temperature Ionic Liquid: Persistent Local Environments and the Red-Edge Effect. *Proc. Natl. Acad. Sci. U.S.A.* **2006**, *103*, 831−836.

(25) Hu, Z. H.; Margulis, C. J. Room-Temperature Ionic Liquids: Slow Dynamics, Viscosity, and the Red Edge Effect. *Acc. Chem. Res.* **2007**, *40*, 1097−1105.

(26) Hu, Z. H.; Margulis, C. J. A Study of the Time-Resolved Fluorescence Spectrum and Red Edge Effect of ANF in a Room-Temperature Ionic Liquid. *J. Phys. Chem. B* **2006**, *110*, 11025−11028.

(27) Mandal, P. K.; Sarkar, M.; Samanta, A. Excitation Wavelength Dependent Fluorescence Behavior of the Room Temperature Ionic Liquids and Dissolved Dipolar Solutes. *J. Phys. Chem. A* **2004**, *108*, 9048−9053.

(28) Samanta, A. Dynamic Stokes Shift and Excitation Wavelength Dependent Fluorescence of Dipolar Molecules in Room Temperature Ionic Liquids. *J. Phys. Chem. B* **2006**, *110*, 13704−13716.

(29) Böhm, V. P. W.; Herrmann, W. A. The "Wanzlick Equilibrium". *Angew. Chem., Int. Ed.* **2000**, *39*, 4036−4038.

(30) Seddon, K. R.; Stark, A.; Torres, M. J. Influence of Chloride, Water, and Organic Solvents on the Physical Properties of Ionic Liquids. *Pure Appl. Chem.* **2000**, *72*, 2275−2287.

(31) Huddleston, J. G.; Visser, A. E.; Reichert, W. M.; Willauer, H. D.; Broker, G. A.; Rogers, R. D. Characterization and Comparison of Hydrophilic and Hydrophobic Room Temperature Ionic Liquids Incorporating the Imidazolium Cation. *Green Chem.* **2001**, *3*, 156−164.

(32) Wang, J. J.; Tian, Y.; Zhao, Y.; Zhuo, K. A Volumetric and Viscosity Study for the Mixtures of 1-*n*-butyl-3-methylimidazolium Tetrafluoroborate Ionic Liquid with Acetonitrile, Dichloromethane, 2-Butanone and *N,N*-dimethylformamide. *Green Chem.* **2003**, *5*, 618−622.

(33) Zhu, J. Q.; Chen, J.; Li, C. Y.; Fei, W. Y. Viscosities and Interfacial Properties of 1-Methyl-3-butylimidazolium Hexafluorophosphate and 1-Isobutenyl-3-methylimidazolium Tetrafluoroborate Ionic Liquids. *J. Chem. Eng. Data* **2007**, *52*, 812−816.

(34) Baker, S. N.; Baker, G. A.; Kane, M. A.; Bright, F. V. The Cybotactic Region Surrounding Fluorescent Probes Dissolved in 1-Butyl-3-methylimidazolium Hexafluorophosphate: Effects of Temperature and Added Carbon Dioxide. *J. Phys. Chem. B* **2001**, *105*, 9663−9668.

(35) Triolo, A.; Russina, O.; Bleif, H. J.; Di Cola, E. Nanoscale Segregation in Room Temperature Ionic Liquids. *J. Phys. Chem. B* **2007**, *111*, 4641−4644.

(36) Canongia Lopes, J. N. A.; Pádua, A. A. H. Nanostructural Organization in Ionic Liquids. *J. Phys. Chem. B* **2006**, *110*, 3330−3335.

(37) Bowers, J.; Butts, C. P.; Martin, P. J.; Vergara-Gutierrez, M. C.; Heenan, R. K. Aggregation Behavior of Aqueous Solutions of Ionic Liquids. *Langmuir* **2004**, *20*, 2191−2198.

(38) Noda, A.; Hayamizu, K.; Watanabe, M. Pulsed-Gradient Spin−Echo ^{1}H and ^{19}F NMR Ionic Diffusion Coefficient, Viscosity, and Ionic Conductivity of Non-Chloroaluminate Room-Temperature Ionic Liquids. *J. Phys. Chem. B* **2001**, *105*, 4603−4610.

(39) Tokuda, H.; Hayamizu, K.; Ishii, K.; Abu Bin Hasan Susan, M.; Watanabe, M. Physicochemical Properties and Structures of Room Temperature Ionic Liquids. 1. Variation of Anionic Species. *J. Phys. Chem. B* **2004**, *108*, 16593−16600.

(40) Tokuda, H.; Hayamizu, K.; Ishii, K.; Susan, M. A. B. H.; Watanabe, M. Physicochemical Properties and Structures of Room Temperature Ionic Liquids. 2. Variation of Alkyl Chain Length in Imidazolium Cation. *J. Phys. Chem. B* **2005**, *109*, 6103−6110.

(41) Umecky, T.; Kanakubo, M.; Ikushima, Y. Self-Diffusion Coefficients of 1-Butyl-3-methylimidazolium Hexafluorophosphate with Pulsed-Field Gradient Spin-Echo NMR Technique. *Fluid Phase Equilib.* **2005**, *228*, 329−333.

(42) Morrow, T. I.; Maginn, E. J. Molecular Dynamics Study of the Ionic Liquid 1-*n*-Butyl-3-methylimidazolium Hexafluorophosphate. *J. Phys. Chem. B* **2002**, *106*, 12807−12813.

(43) Kowsari, M. H.; Alavi, S.; Ashrafizaadeh, M.; Najafi, B. Molecular Dynamics Simulation of Imidazolium-Based Ionic Liquids. I. Dynamics and Diffusion Coefficient. *J. Chem. Phys.* **2008**, *129*, 224508.

(44) Hussey, C. L.; Sun, I. W.; Strubinger, S. K. D.; Barnard, P. A. Some Observations about the Diffusion Coefficients of Anionic Transition Metal Halide Complexes in Room-Temperature Haloaluminate Ionic Liquids. *J. Electrochem. Soc.* **1990**, *137*, 2515−2516.

(45) Tracy, M. A.; Garcia, J. L.; Pecora, R. An Investigation of the Microstructure of a Rod Sphere Composite Liquid. *Macromolecules* **1993**, *26*, 1862−1868.

(46) Wang, Y. T.; Voth, G. A. Unique Spatial Heterogeneity in Ionic Liquids. *J. Am. Chem. Soc.* **2005**, *127*, 12192−12193.